Energy 211 (2020) 118996

Contents lists available at ScienceDirect

Energy

journal homepage: www.elsevier.com/locate/energy

Biowaste to hydrogen or Fischer-Tropsch fuels by gasification – A Gibbs energy minimisation study for finding carbon capture potential and fossil carbon displacement on the road

Norbert Lümmen*, Erlend Velken Røstbø

Department of Mechanical and Marine Engineering, Western Norway University of Applied Sciences, Postboks 7030, 5020, Bergen, Norway

ARTICLE INFO

Article history:
Received 14 July 2020
Received in revised form
13 September 2020
Accepted 2 October 2020
Available online 7 October 2020

Keywords:
Biowaste
Gasification
Gibbs energy minimisation
Hydrogen
Fischer-Tropsch fuels

ABSTRACT

To reach its greenhouse gas emission reduction goals, Norway needs a shift away from the use of fossil fuels in the transport sector. The production potential and efficiency of Fischer-Tropsch biofuels and hydrogen from gasified wet organic municipal solid waste has been investigated. The carbon capture potential was estimated for both production processes and the number of road vehicles compared, which can be supplied with the fuel. Gibbs free energy minimisation is used to predict the synthesis gas composition. A detailed analysis of the different gas treatment processes that lead to either gasoline and diesel production, along with energy recovery as electricity, or hydrogen in either compressed or liquefied form is conducted. Both processes can utilise all available waste heat and the Fischer-Tropsch biofuel process is even self-sufficient with electrical power. The production of hydrogen has both higher first and second law efficiencies and a greater number of vehicles can be supplied with fuel. Either 2367 tonne H_2 or 1497 tonne gasoline, 1279 tonne diesel, and 1.33 MW of net electric power can be produced at 1073 K gasification temperature, where both yield and efficiencies are highest. Hydrogen production also has the larger carbon capture potential during fuel production.

1 Introduction

In 2019, 50.3 million tonne CO_2 equivalents were emitted to the atmosphere from Norwegian territories of which 42.2 million tonne were CO_2 [1]. While this amount appears to be negligible on a global scale (0.12% of global CO_2 emissions in 2018 [2]), the Norwegian government has committed to reductions in greenhouse gas emissions to 60% of the level produced in 1990, or less, by the year 2030 [3]. A reduction by 20 million tonne CO_2 equivalents is necessary by the end of this decade to reach these goals when the values for 2019 are used as reference. The transport sector has great potential to contribute to the necessary reductions. 16.8 million tonne CO_2 equivalents were emitted by road traffic, domestic aviation, navigation, fishing, and motor equipment in 2018 [1], of which 13.2 million tonne were CO_2. By realising carbon emission free transport in Norway until 2030, 84% of the necessary reduction of greenhouse gas emissions could be achieved by this sector alone. Road traffic could account for a reduction of 9.1 million tonne CO_2 equivalents or 45.5% of the necessary reductions. At the beginning of 2020, ca. 9.3% of all private cars were electric, an increase of 33.4% from the previous year. The heavy part of the road transport sector (vans, buses, light and heavy trucks) is proving more difficult to electrify due to the necessary battery capacity and the weight penalty it brings with it. The same applies to marine and aerial transport, even though electric solutions for small planes (up to nine passengers) are under investigation. Otherwise, the focus in these sectors is on hydrogen, ammonia, and biofuels.

Due to the abundance of hydropower in Norway, the production of hydrogen, ammonia and other electro fuels using this natural energy source for electrolysis is under investigation for local and regional production, use and export. Offshore wind power is being considered for the same purposes. The storage of CO_2 resulting from hydrogen production from fossil sources is also a possibility, which can utilise old oil and gas wells on the continental shelf. This is an option for using fossil energy carriers with potentially very limited fossil carbon emissions to the atmosphere.

In 2018, the potential mass of organic material for chemical energy recovery to fuels available in Norway was 1.77 million tonne from wood waste, wet organic waste, sludge, and garden and park

* Corresponding author.
E-mail address: nlu@hvl.no (N. Lümmen).

https://doi.org/10.1016/j.energy.2020.118996

Nomenclature

Abbrevation/symbol	Meaning
ASF	Andersen-Schulz-Flory
BG	biomass gasification
CCS	carbon capture and storage
CCUS	carbon capture, use, and storage
FT	Fischer-Tropsch
LT	low temperature
HT	high temperature
HHV	higher heating value
HX	heat exchanger
K.O.	knock out
LHV	lower heating value
MEA	monoethanolamine
NREL	National Renewable Energy Lab
PSA	pressure swing adsorption
RMSE	root mean square error
SNG	synthetic natural gas
VLE	vapour-liquid equilibrium
WGS	water-gas shift
ZnO	zinc oxide
ar	as received
compr	compressed
dry	on dry basis
daf	dry and ash free
el	electric
liq	liquid
$\overline{G}$	molar Gibbs free energy
$\Delta\overline{G}^{o}_{f,i}$	molar Gibbs free energy of formation of compound i
$\Delta\overline{H}^{o}_{f,i}$	molar enthalpy of formation of compound i
$\overline{H}^{o}$	molar enthalpy
$\dot{m}$	mass flow rate
m	number of carbon atoms
n	amount of substance
P	pressure
$\overline{Q}_{loss}$	heat loss from the gasifier
R	universal gas constant
$\Delta\overline{S}^{o}_{f,i}$	molar entropy of formation of compound i
T	temperature
$\dot{W}$	power
x_{chem}	specific chemical exergy
y_i	mole fraction of compound i
α	chain growth factor
η_I	energy efficiency, first law efficiency
η_{II}	exergy efficiency, second law efficiency
μ_i	chemical potential of compound i
ψ	specific thermal exergy

waste [4]. However, only 0.23 million tonne of biogas was produced from these waste fractions; mainly from wet organic waste and sludge [4]. The potential production of Fischer-Tropsch (FT) fuels from air-captured CO_2 or from the carbon content in synthesis gas (syngas) from gasified biomass has so far received little attention. Hydrogen production potential from gasified wet organic waste in the Bergen region in Western Norway was estimated by one of the authors [5]. The estimate was based on the syngas composition as calculated by Gibbs energy minimisation and the resulting hydrogen and carbon monoxide content. The latter was used to estimate the possible increase in hydrogen production potential by using the water-gas shift reaction. However, this estimate did neither consider the details and energy needs of the specific processes of syngas upgrading to hydrogen when calculating energy and exergy efficiencies nor the energy need for providing compressed or liquid hydrogen to potential customers.

The aim of the current work is to compare the production potential of both hydrogen and FT biofuels from the same wet organic feedstock through an analysis of the first and second law efficiencies. Additionally, the types and prevalence of various classifications of road transport vehicles will be considered with the goal of estimating the related CO_2 capture and displacement potential. This will be in the context of modelling the production process, which is made in a more refined manner than detailed in a previous study on hydrogen production [5]. This more detailed analysis considers the energy need in feedstock preparation ahead of the gasification and other processes, and a greater variety of product compounds in the gasification process; as well as including the ash content in the energy balance. Changes in the syngas composition in the gas cleaning and treatment, ahead of hydrogen separation or FT biofuel production, are accounted for as are the utilisation of the respective offgases and waste heat integration.

Wright et al. conducted a techno-economic analysis of biomass fast pyrolysis to transportation fuels (naphtha and diesel) for a scenario which considered the processing of 2000 dry tonne per day of corn stover [6], which is about 20 times the amount of waste to be processed in this study. The fuel prices obtained were found to be competitive with those from fossil feedstock. Wang et al. studied the sustainable design and synthesis of a hydrocarbon biorefinery based on gasification [7] by life cycle assessment and a multi-objective techno-economic analysis: the products were gasoline and diesel. The optimal solution regarding environmental and economic performance was found to involve, amongst others, high temperature gasification, internal hydrogen production and using a cobalt catalyst in the Fischer-Tropsch synthesis. The National Renewable Energy Laboratory (NREL) in the US, has published a number of reports on biomass gasification and production of both hydrogen [8] and Fischer-Tropsch biofuels [9] from the available syngas. Both studies were for large plants (2000 dry tonne biomass per day) and included current and goal designs for the complete production process, along with assessments of heat integration and economic feasibility. Doranehgard et al. [10] have developed a semi-kinetic Aspen Plus model for studying hydrogen production with in-situ CO_2 capture based on biomass gasification. Howaniec & Smoliński [11] studied the effect of fuel blend composition on the efficiency of hydrogen-rich gas production in co-gasification of coal and biomass. Their steam co-gasification process of coal and biomass for efficient hydrogen generation showed an increase in total gas and hydrogen yields.

Im-orb et al. investigated the Fischer-Tropsch biofuel synthesis from rice straw by techno-economic [12] and techno-environmental analyses [13]. The former of which studied the effect of Fischer-Tropsch (FT) offgas recirculation on the product yield with the Aspen Custom Modeler program. A high CO conversion rate of 98% could be achieved even without recirculation of the off gas, and was just dependent on FT reactor size; but the syngas and fuel production rates could be optimised by tuning the recycle fraction and FT reactor volume. The follow-up work in Refs. [13] studied the effect of different process configurations in the biomass to liquid and electricity process. The configuration involving auto-thermal reforming was found to be the most suitable one as it offered maximum heat recovery and minimum external utility

requirement. A study conducted by Barbuzza et al. [14] investigated the use of hydrogen produced by solar and wind energy in a woody biomass gasification process for the production of synthetic natural gas (SNG). They were able to show that SNG generated in this way represents an efficient means for renewable energy storage. Cruz et al. [15] conducted an exergy analysis of alternative configurations of a system coproducing synthetic fuels and electricity via biomass gasification, Fischer-Tropsch synthesis and a combined-cycle scheme. The exergy efficiency of the whole system was reported to be around 25%. Process efficiency of biofuel production via gasification and Fischer–Tropsch synthesis was studied by Leibbrandt et al. in 2013 [16]. They obtained a maximum overall process efficiency of 51%, of which 40% was in the form of Fischer–Tropsch liquids.

This article is structured as follows: Section 2 lists the properties of the biomass that is the basis for the following calculations. In section 3, the suggested production processes for the Fischer-Tropsch biofuels and hydrogen are introduced. The gasification equation and Gibbs energy minimisation routine are discussed before the workflow and calculations of efficiencies are described. The results concerning the fuel production potential, efficiencies and CO_2 reduction potential are presented in section 4, and discussed in Section 5. The conclusion in section 6 rounds up this work.

2 Data

The municipal solid waste from the Bergen region has been analysed in earlier work [17,18]. The hydrogen production potential from different waste fractions was estimated in previous work as well [5], but not in such detail as presented here. For this study, the combined (industrial and household) wet organic waste fraction has been selected. The waste properties are listed in Table 1 (parts of proximate analysis), Table 2 (ultimate analysis) and Table 3 (heating value and specific exergy). Table 3 also contains data for gasoline, diesel, and hydrogen, which is used for efficiency calculations.

3 Methods

The suggested production methods for both hydrogen and FT fuels from gasified biomass are discussed in the following subsections. They are identical from preparation of the biomass to the inlet of the syngas compressor. The setup is based on the biomass gasification processes suggested by Spath et al. [8] for hydrogen and Swanson et al. [9] for Fischer-Tropsch biofuel production. The syngas cleaning part is based on a further report published by the National Renewable Energy Laboratory [19]. Temperatures and pressures of the different states were taken from these reports where it was not necessary or possible to calculate temperatures based on energy balances.

Table 1
Wet organic waste mass, moisture, and ash content (ar: as received; dry: on dry basis; daf: dry and ash free).

biomass	mass/tonne
mass (ar)	54,266
moisture	18,423
mass (dry)	35,843
ash	9,285
mass (daf)	26,558

Table 2
Ultimate analysis of the wet organic waste (ar: as received; dry: on dry basis).

compound	C	H	O	N	S	ash	moisture
wt% (ar)	24.7%	3.1%	19.7%	1.1%	0.3%	17.1%	33.9%
wt% (dry)	37.5%	4.7%	29.8%	1.6%	0.5%	25.9%	

Table 3
Lower heating value (LHV), chemical exergy and density (where available) for biomass, gasoline, diesel, and hydrogen.

property	biomass (dry)	gasoline	diesel	hydrogen
LHV / kJ/kg	12,546	44,000	43,200	120,000
x_{chem} / kJ/kg	15,759	47,394	44,400	117,108
ρ / kg/m^3	(not available)	755	840	0.0899

3.1. Fischer-Tropsch fuel production

Fig. 1 shows the process flow chart of the suggested production process of Fischer-Tropsch fuels. A shredder reduces the size of the wet organic waste as a first of three steps in feed preparation before it is dried to 10 wt% moisture content, and finally further ground to millimetre size before it enters the downdraft gasifier. The syngas leaving the gasifier is cleaned from particles and fly ash in a cyclone separator. Char is also collected in the cyclone separator and incinerated in a separate char combustor (not shown). The thermal energy in the flue gas is used for heating in, for example, the biomass drying process. A tar reformer cracks larger hydrocarbons prior to the syngas being cooled down, before a wet scrubber washes out remaining tars and fine particles. The syngas is saturated with steam when it enters the sour gas treatment. Monoethanolamine (MEA) is used to separate both H_2S and CO_2 from the syngas. The sulphur content is separated further in a LO-CAT® process. A five-stage compressor with intercooling raises the pressure in the syngas to 24 bar. The compressed syngas is heated to 473 K with heat available from syngas cooling before the sulphur content is further reduced in a ZnO reactor to the maximum allowed (0.2 ppm) in the following water-gas shift (WGS) reactor. Steam is added to the syngas to adjust the H_2/CO-ratio to 2.37, which was mentioned as an optimum value by Im-Orb et al. [12]. The water-gas shift reaction is also employed in the hydrogen production process (see section 3.2). Using a catalyst, CO is converted to CO_2 by transferring an oxygen atom from a water molecule to a CO molecule, leaving a hydrogen molecule behind. The reaction formula of this moderately exothermic process (41.1 kJ/mol [20]) is

$$CO + H_2O \rightarrow CO_2 + H_2 \quad (1)$$

After the H_2/CO-ratio adjustment, the syngas temperature is once more adjusted to the desired temperature in the Fischer-Tropsch reactor, where a cobalt-based catalyst is used. Liquid hydrocarbons, water and the gas phase are separated. The gas phase is combusted with compressed air and expanded to atmospheric pressure in a gas turbine. Flue gas from the turbine exit is mixed with the flue gas from the char combustion and sent to a second CO_2 separation process. The liquid hydrocarbons leaving the FT reactor are subject to further processing, which can involve pressure reduction, separation into gasoline and diesel fractionation etc. (not shown in detail here).

3.2. Hydrogen production

The beginning of the hydrogen production process studied (see Fig. 2) is identical to the one for FT fuel production (see section 3.1) from the start of the biomass shredding to the inlet of the five-stage compressor with intercooling. The compressor raises the pressure

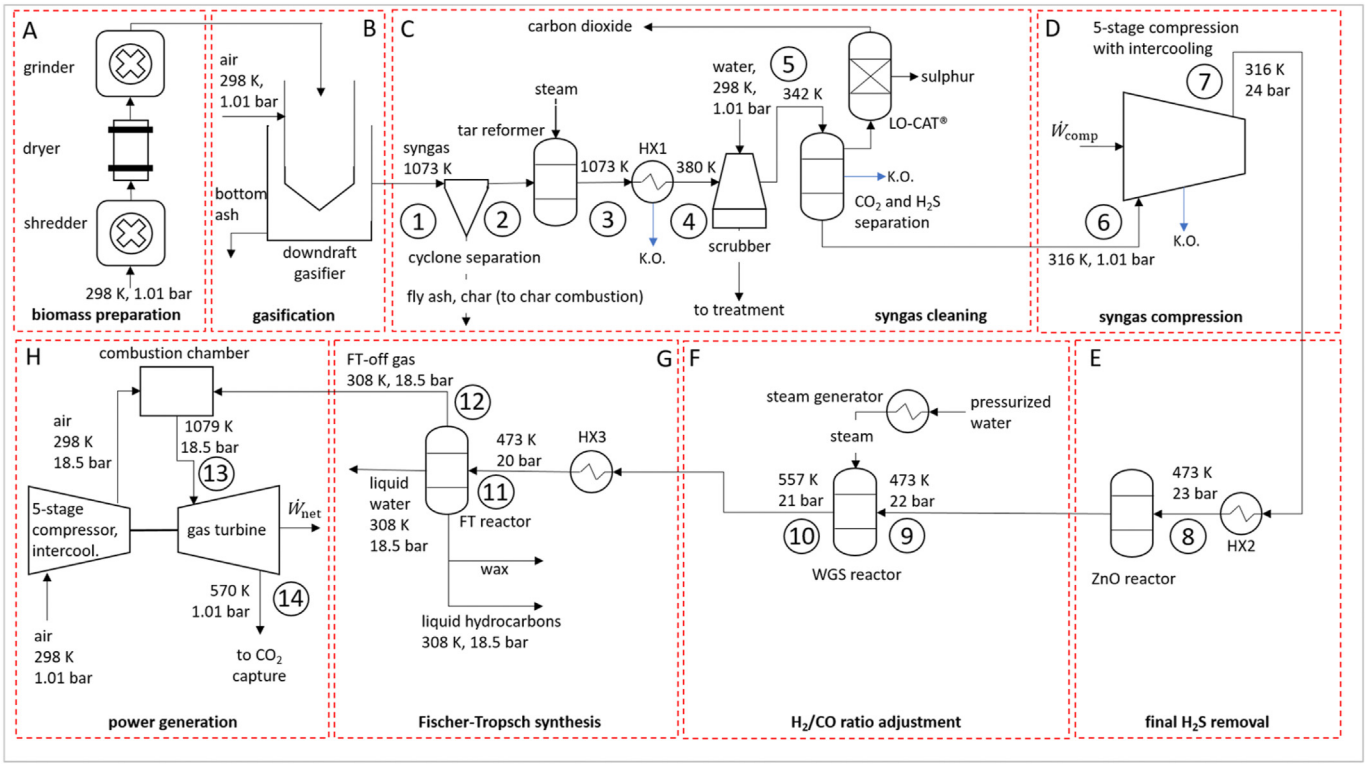

Fig. 1. Flow chart of the process to produce Fischer-Tropsch biofuels by biomass gasification at 1073 K gasification temperature.

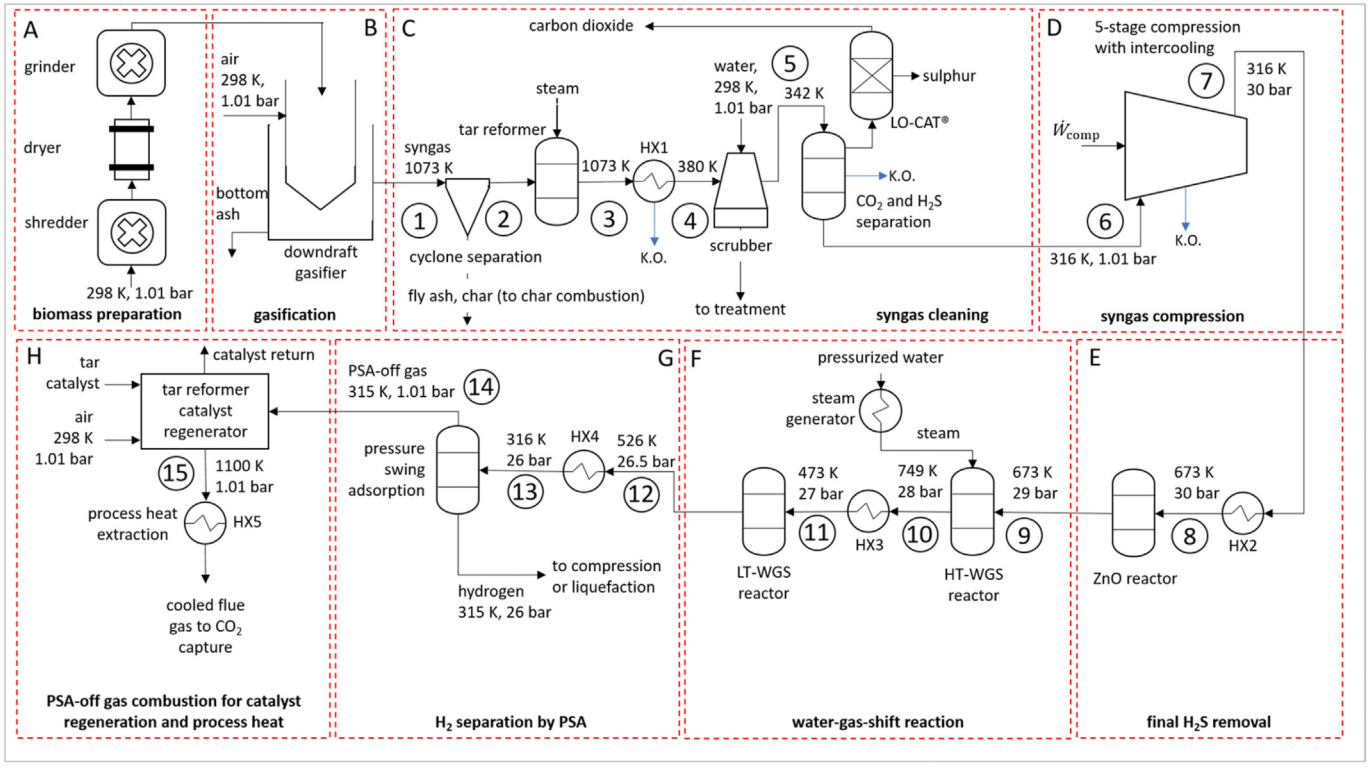

Fig. 2. Flow chart of the process to produce hydrogen by biomass gasification at 1073 K gasification temperature.

to 30 bar in this case, which is higher than in the FT fuel production process. After the compressor, the syngas is heated up to 673 K for H_2S reduction in the ZnO reactor (to max. 0.2 ppm H_2S). Steam is provided to the following high temperature (HT) and low temperature (LT) WGS reactors which reach a total CO conversion factor of 0.98 [8]. A heat exchanger between the two WGS reactors adjusts

the temperature to 473 K before the LT-WGS reactor. The WGS reaction is favourable at low temperatures. However, the reaction rates diminish at low temperatures. The reaction is therefore often carried out in two adiabatic steps and at different inlet temperatures in order to maximise the CO conversion [20]. There are also different types of catalysts used at the two different temperature levels. These may be iron oxide, chromium oxide based catalysts in the high temperature reactor and copper oxide in a mixture with zinc oxide catalysts in the low temperature reactor [8].

The following pressure swing absorption (PSA) unit separates 90% of the H_2 content in the syngas. PSA is an automated batch process for gas separation. Near continuous flow can be achieved by operating several sub-units in parallel. Due to the use of air as gasification medium, the mole fraction of hydrogen in the produced gas is about 34% prior to separation. According to Spath et al. [8], this is too low for economic efficient direct separation. However, using a PSA unit with recirculation to the input flow to the unit, large enough mole fractions can be realised in order to achieve an economic separation process and high hydrogen purity.

The high purity hydrogen gas flow can then be further compressed (350 bar) or liquefied if needed. The PSA offgas is mixed with air and combusted, and the thermal energy in the flue gas used to both regenerate the tar reformer catalyst and provide process heat otherwise. In addition to the CO_2 captured from the syngas, char and PSA offgas combustion provide a further gas flow for additional CO_2 separation.

3.3. Syngas composition calculations

The composition of the syngas leaving the gasifier is estimated by means of Gibbs energy minimisation of the products of the gasification reaction (excluding the solid compounds char and ash) following the algorithm presented in Ref. [5]. The algorithm is implemented in Matlab where the fmincon() function is applied for the minimisation. The gasification reaction equation is

$$\begin{aligned}&CH_yO_zN_aS_b + wH_2O + r(O_2 + 3.76N_2) + n_{CaO}CaO(s)\\&\quad + n_{SiO_2}SiO_2(s) \Leftrightarrow n_{H_2}H_2 + n_{CH_4}CH_4 + n_{CO}CO + n_{CO_2}CO_2\\&\quad + n_{NH_3}NH_3 + n_{NO}NO + n_{NO_2}NO_2 + n_{N_2O}N_2O + n_{C_2H_2}C_2H_2\\&\quad + n_{C_2H_4}C_2H_4 + n_{C_6H_6}C_6H_6 + n_{H_2O}H_2O + n_{N_2}N_2 + n_{SO_2}SO_2\\&\quad + n_{H_2S}H_2S + n_C C(s) + n_{CaO}CaO(s) + n_{SiO_2}SiO_2(s)\end{aligned} \tag{2}$$

This equation has been extended by the addition of several compounds among the products and the inclusion of ash on both sides compared with its earlier version in ref. [5] (to which the reader is referred for details), which was based on the work by Fournel et al. [21]. The coefficients y, z, a, b, w, n_{CaO} and n_{SiO_2} are calculated based on the waste properties. The coefficient r is calculated by the aforementioned Matlab algorithm to satisfy the specified gasification temperature and w is the moisture content per kilomole biomass. According to Fournel et al. [21], ash can be assumed to consist of equal parts (50 wt%) CaO and SiO_2. The ash is inert in the gasification process; but like char, it removes some thermal energy from the process, which is not available to the syngas producing reactions that would otherwise happen in the various zones of the gasifier. It was therefore added to both sides of the energy balance which needs to be satisfied along with the mass balances of each element.

The n_i on the right hand side of equation (2) are to be determined by minimizing the molar Gibbs energy $\overline{G}$ of the products under certain assumptions and constraints, similar to the works of Fournel et al. [21] and Jarungthammachote and Dutta [22,23].

It is assumed that the process is a steady flow process where the moisture-reduced biomass and dry atmospheric air enter the reaction volume in separate streams at 25°C and 1 atm. The residence time in the reaction volume is assumed to be long enough to reach chemical equilibrium before the reaction products leave the gasifier.

A further assumption is that the gaseous reaction products can be treated as a mixture of ideal gases. Since about 50% of the sulphur content of the biomass may be contained in the ash in combustion products [21], the same is assumed for gasification [24]. The corresponding elemental mass balance will therefore only take $0.5b$ into account among the gaseous products (H_2S and SO_2). The heat loss $\overline{Q}_{loss}$ from the gasifier is set to 1% of the higher heating value of the biomass by default as is typical for industrial sized and operated gasifiers [25].

At thermodynamic equilibrium, the Gibbs energy of a system is minimal. Being constrained only by the conservation of the total mass input to the reaction and the mass conservation of each element, the total molar Gibbs energy $\overline{G}$ of the gasification products (right hand side of equation (2)) is minimized

$$\overline{G} = \sum_{i=\text{species}} n_i \mu_i \tag{3}$$

Here, μ_i is the chemical potential of product species i and calculated by

$$\mu_i = \Delta\overline{G}^{o}_{f,i} + RT\ln y_i \tag{4}$$

for the gaseous product species. $\Delta\overline{G}^{o}_{f,i}$ is the standard Gibbs free energy of formation of species i at the equilibrium temperature T and pressure P (= 1 atm). It is zero for all elements regardless of the value of T. R is the universal gas constant and y_i is the mole fraction of (gaseous) species i, where

$$y_i = n_i \Big/ n_{\text{total,gas.prod.}} \tag{5}$$

and

$$n_{\text{total,gas.prod.}} = \sum_{i=\text{gas. products}} n_i \tag{6}$$

Using equations (5) and (6), equation (3) can be written as

$$\overline{G} = \sum_{i=\text{species}} n_i \left(\Delta\overline{G}^{o}_{f,i} + RT\ln y_i \right) \tag{7}$$

$\overline{G}$ is to be minimized under the constraints that

$$0 \le n_i \le n_{\text{total}} \tag{8}$$

and that the n_i fulfill the conservation of mass for the elements.

In order to find the minimum value of $\overline{G}$, the n_i are varied by the fmincon() function, which is part of the optimization toolbox in MATLAB® (version 2019b (9.7.0.1319299, update 5), The MathWorks, Natick, MA, USA), under the mentioned constraints. The necessary $\Delta\overline{G}^{o}_{f,i}$ values of the product species are calculated with [21]

$$\Delta\overline{G}^{o}_{f,i} = \Delta\overline{H}^{o}_{f,i} - T\Delta\overline{S}^{o}_{f,i} \tag{9}$$

following the calculation of these properties outlined in and with data from the NASA Technical Memorandum 4513 [26].

The energy balance of the steady process in the gasifier is an

important part of the chosen method. It is used to obtain the actual equilibrium temperature of the process at a given set of n_i and values of r and w. It can be written as follows

$$\sum_{r=\text{reactants}} n_r \overline{H}_r^{o}(T_0) = \sum_{p=\text{products}} n_p \overline{H}_p^{o}(T) + \overline{Q}_{\text{loss}} \quad (10)$$

$\overline{Q}_{\text{loss}}$ is the heat loss from the surface of the control volume (gasifier) due to imperfect thermal insulation. $\overline{H}_r^{o}(T_0)$ and $\overline{H}_p^{o}(T)$ are the enthalpies of the reactants and products at their respective temperatures. The amount of air input to the gasification reaction is varied until the required gasification temperature T balances equation (10). A graphic representation of the algorithm can be found in ref. [5]. Other energy balances used in this work are constructed in a similar way as equation (10) with terms for added heat or produced shaft work depending on the specific process.

A validation of the improved Matlab code was conducted using the same experimental results [27] as reference as in earlier work [5]. Table 4 shows that the inclusion of ash into the energy balance has actually decreased the root mean square error (RMSE) calculated for the mole fractions for five of the important compounds in the syngas for the reference fuel (sawdust; ref. [27]) used in the development of the code for earlier work by the authors [5] and others [21,22].

Gasification processes can reach carbon conversion ratios of up to 98%. A value of 95% conversion of the carbon content in the biomass to gaseous compounds in the syngas has been assumed in this work. The other 5% leave the gas flow in the cyclone separator, are subsequently combusted and the thermal energy of the flue gases utilized.

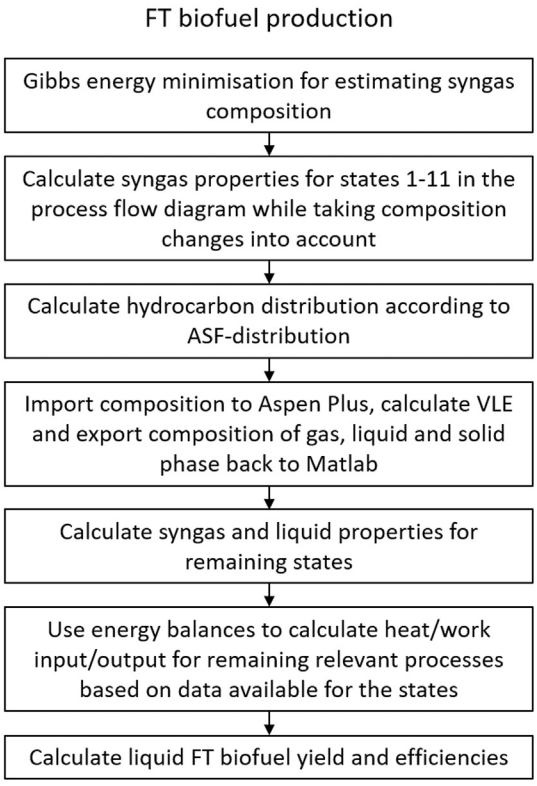

Fig. 3. Workflow for the FT biofuel production potential calculations.

3.4. Workflow

The work flow of the calculations for FT biofuel and hydrogen production potential are sketched in Fig. 3 and Fig. 4.

The calculations of both hydrogen and FT biofuel production potential, along with their energy and exergy efficiencies, begin with the Gibbs energy minimisation calculations of the syngas composition for biomass at 10 wt% moisture after drying in a first Matlab script. Based on this initial composition, syngas properties are calculated for the different states in the process flow charts (Figs. 1 and 2) by means of a second Matlab script, which utilises the same routine for calculating the thermal properties of the involved chemical compounds [26]. Results are stored in a Microsoft Excel sheet. Changes in composition are accounted for whenever chemical reactions occur between two states: cooling leads to condensation of steam or substances like MEA remove CO_2 and H_2S from the syngas for example.

The power demand for shredder and grinder were taken from the work of Swanson et al. [9]. The syngas compressors are treated as 5-stage compressors with intercooling (to 43°C). Each stage is assumed to have an isothermal efficiency of 80%. The compressor used to raise the pressure in the combustion air for FT offgas combustion is assumed to be a 4-stage compressor with 75% isentropic efficiency. The hydrogen compressor has an isothermal efficiency of 72%. An isentropic efficiency of 85% was used for calculating the power output of the gas turbine expanding the combusted FT offgas. The generator efficiency used for calculating the electric power output was set to 98%.

Temperatures in combustion processes are calculated as adiabatic flame temperatures. Mass and energy flows, as well as efficiencies, are calculated from the data for the different states stored in the Excel file. In case of the FT fuels, the separation into gaseous and liquid streams is carried out in Aspen Plus V10 using the Peng-Robinson equation of state for solving the vapour-liquid equilibrium (VLE). For this, data is transferred from the Excel sheet to Aspen and back to it after the VLE is solved. The Matlab script then

Table 4
Mole fraction and root mean square error (RMSE) for the five most important compounds in the syngas produced from sawdust by Altafini et al. [27] and compared to models developed by other groups [21,22]. 'Exp.' stands for experimental results, 'simple' (model) means that there is no constraint on the value for methane while 'modified' means that the mole fraction of methane is fixed to the specified amount given in the table.

	Altafini (2003)		Jarungthammachote (2007)	Fournel (2015)		this work		
	Exp.	Model	Modified	Simple	Modified	Simple	Modified	Modified
vol% H_2	14.00	20.06	18.24	21.69	18.83	19.65	17.84	17.12
vol% CO	20.14	19.70	23.34	23.46	21.47	20.84	20.70	20.69
vol% CH_4	2.31	0.00	1.66	0.03	1.66	0.02	1.66	2.31
vol% CO_2	12.06	10.25	9.82	9.57	11.14	10.82	11.44	11.67
vol% N_2	50.79	50.10	46.93	45.26	46.90	48.66	48.36	48.21
RMSE		3.03	3.12	4.74	2.88	2.96	2.09	1.84
H_2/CO	0.695	1.018	0.781	0.925	0.877	0.943	0.861	0.828
H_2/CO deviation		46%	12%	33%	26%	36%	24%	19%

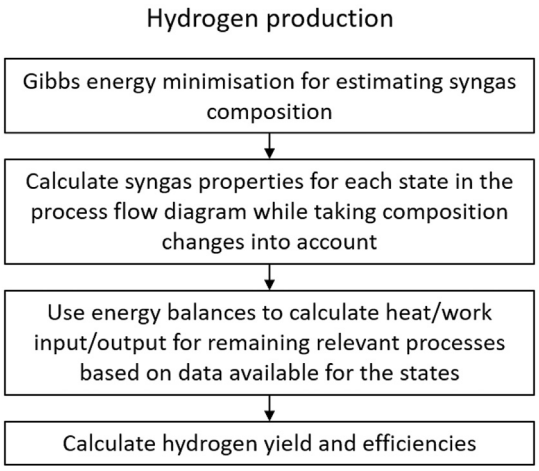

Fig. 4. Workflow for the hydrogen production potential calculations.

continues calculating the properties in the states following the FT reactor and writing the properties obtained to further sheets in the Excel file.

After production, the liquid Fischer-Tropsch products are further expanded to surroundings pressure (1.01 bar absolute) and separated into gaseous and liquid phases. This final liquid phase is then divided into gasoline (CH_4–$C_{11}H_{24}$) and diesel ($C_{12}H_{26}$–$C_{20}H_{42}$). The waxes, modelled as $C_{30}H_{62}$, are neglected in the further analysis of the Fischer-Tropsch fuel production and assumed to be further processed to other products in another facility.

The Matlab scripts make use of the CoolProp extension [28] (version 6.1) whenever the amount of knock out water needs to be calculated.

3.5. Syngas post-processing

After its initial production, the syngas is subject to many different processes that change both its pressure, temperature, and chemical composition. Table 5 lists the used conversion factors and degree of compound removal for the different processes.

The conversion of CO and H_2 to hydrocarbons is modelled by means of the Andersen-Schulz-Flory (ASF) distribution and gives the mole fractions of the alkanes with m carbon atoms produced from the converted CO and H_2 [12].

$$y_{C_mH_{2m+2}} = \alpha^{m-1}(1-\alpha) \tag{11}$$

The chain growth factor α is calculated with the following equation for the suggested Co-based catalyst [7,9].

$$\alpha = \left[0.2332\frac{y_{CO}}{y_{CO}+y_{H_2}} + 0.6330\right]\cdot[1 - 0.0039(T_{FT} - 533\ \mathrm{K})] \tag{12}$$

where T_{FT} is the temperature in during the Fischer-Tropsch synthesis and y_{CO} and y_{H_2} are the mole fractions of CO and H_2 at the inlet to the Fischer-Tropsch reactor, respectively. Calculations for T_{FT} values of 473 K and 493 K have been made to study its effect on the FT fuel production.

3.6. Calculation of efficiencies

The energy efficiency of the Fischer-Tropsch fuel production processes with electricity production from combusted FT offgas expansion in a gas turbine is calculated as

$$\eta_{I,LHV,FT} = \frac{\dot{m}_{gasoline}LHV_{gasoline} + \dot{m}_{diesel}LHV_{diesel} + \dot{W}_{el,net}}{\dot{m}_{biomass,dry}LHV_{biomass,dry}} \tag{13}$$

The electric power term in the numerator ($\dot{W}_{el,net}$) is the net electric power after compressor power for the gas turbine's compressor and the electric power need by shredder, grinder, pumps and syngas compressor have been subtracted. The isentropic efficiency of the turbine was set to 85%, the generator efficiency to 98%. The compressors were modelled with five stages and with intercooling; an equal pressure ratio for all stages was used. The necessary compressor power was calculated by means of the mass flow through each stage and the specific isothermal compressor work for each stage, which was corrected by allowing an isothermal efficiency of 80%.

The energy efficiency of the hydrogen production is calculated accordingly as

$$\eta_{I,LHV,H_2} = \frac{\dot{m}_{H_2}LHV_{H_2}}{\dot{m}_{biomass,dry}LHV_{biomass,dry} + \dot{W}_{process} + \dot{W}_{compr./liq.}} \tag{14}$$

where $\dot{W}_{process}$ represents the sum of power supply to shredder, grinder, syngas compressor and pumps for water pressurisation ahead of steam generation, and $\dot{W}_{compr./liq.}$ is the necessary power for compression to 350 bar or liquefaction. The hydrogen compression power is calculated with an isothermal efficiency of 72% [29]. The liquefaction power is based on a specific energy need

Table 5
Conversion factors and degree of removal of various compounds in the various processes the syngas is subject to.

process	compound	factor	type	products	reference
tar reformation	CH_4	80%	conversion	CO_2, H_2	[8]
	C_2H_2	90%	conversion	CO_2, H_2	[8]
	C_2H_4	90%	conversion	CO_2, H_2	[8]
	C_6H_6	99%	conversion	CO_2, H_2	[8]
	NH_3	99%	conversion	N_2, H_2	[19]
scrubber	C_6H_6	100%	removal		[9]
	NH_3	100%	removal		[9]
MEA treatment/CO_2-capture from flue gas	CO_2	90%	removal		[9]
	H_2S	99%	removal		[9]
ZnO reactor	H_2S	reduction to 0.1 ppm	removal	H_2, S (solid)	[9]
Watergas shift (H_2, HT)	CO	64%	conversion	CO_2, H_2	[8]
Watergas shift (H_2, LT)	CO	85%	conversion	CO_2, H_2	[8]
Fischer-Tropsch synthesis	CO	98%	conversion	hydrocarbons, H_2O	[12]
Pressure swing adsorption	H_2	90%	removal		[8]

of 12.5 kWh/kg H_2 [30].

The calculation of the exergy efficiency follows the same approach as the energy efficiency, but lower heating values are replaced by chemical exergies. The thermal exergy does not contribute in the case of the liquid Fischer-Tropsch fuels because they are assumed to be in thermal equilibrium with the surroundings.

$$\eta_{II,FT} = \frac{\dot{m}_{gasoline} x_{chem,gasoline} + \dot{m}_{diesel} x_{chem,diesel} + \dot{W}_{el,net}}{\dot{m}_{biomass,dry} x_{chem,biomass,dry}} \quad (15)$$

For compressed and liquid hydrogen, however, the thermal exergy is also considered as part of the recovered exergy.

$$\eta_{II,H_2} = \frac{\dot{m}_{H_2} (\psi_{H_2} + x_{chem,H_2})}{\dot{m}_{biomass,dry} x_{chem,biomass,dry} + \dot{W}_{process} + \dot{W}_{compr./liq.}} \quad (16)$$

where ψ_{H_2} is the thermal specific exergy at 315 K and 26 bar gauge directly after PSA separation, at surroundings temperature (298 K) and 350 bar gauge pressure in the case of compressed hydrogen and in the saturated liquid state at 1.01 bar absolute pressure in case of liquefied hydrogen.

4 Results

Results on production potential, energy and exergy efficiency of fuel production and the potential for CO_2 capture and displacement of fossil fuels by the fuel produced from biomass are presented in the following sections.

4.1. Fischer-Tropsch biofuel production

Fig. 5 shows the annual production potential of BG-FT gasoline and BG-FT diesel. The production potential is largest at the lowest temperature of 1073 K. The amount of BG-FT diesel exceeds that of the gasoline product by ca. 402,000 kg. At 20 K higher FT synthesis temperature, the amount of BG-FT gasoline exceeds that of the diesel product by 202,000 kg per year as can be seen in Fig. 6.

The consequence of this small increase in FT synthesis temperature results in a significant shift towards lighter products. This is also reflected in the amount of excess electric energy which can be sold to the net or supply further needs in the plant (Fig. 7). This excess energy is again largest at a gasification temperature of 1073 K. 4000 MWh (523 kW) are available at the lower FT synthesis temperature (473 K) and ca. 2.5 times this amount (10,600 MWh, 1.33 MW) at the higher temperature (493 K).

Fig. 8 shows the efficiency of the combined FT biofuel and electricity production process as a function of gasification temperature (horizontal axis) and FT synthesis temperature (indicated in the line description).

The first law efficiency is given based on the lower heating value of the biomass and the FT products (equation (13)). The values are larger for the higher FT synthesis temperature but decrease with increasing gasification temperature (from 31.1% to 27.8% at 473 K and 35.5% to 31.7% at 493 K).

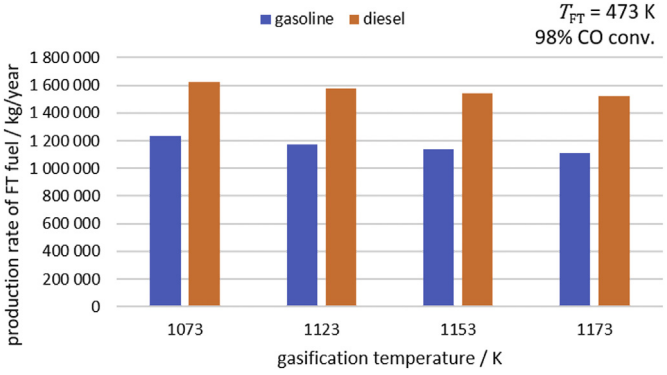

Fig. 5. Annual BG-FT fuel production potential at different gasification temperatures. The CO conversion factor in the FT synthesis is 98% and the FT synthesis temperature is 473 K.

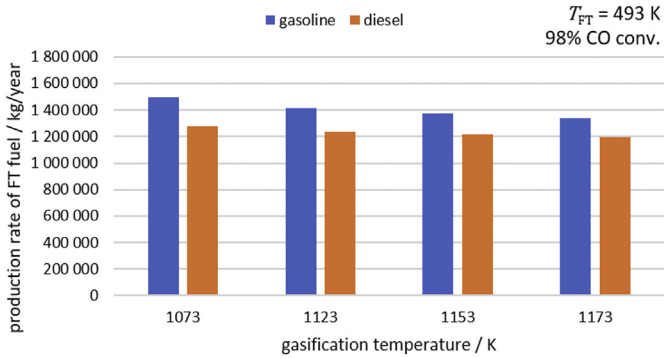

Fig. 6. Annual BG-FT fuel production potential at different gasification temperatures. The CO conversion factor in the FT synthesis is 98% and the FT synthesis temperature is 493 K.

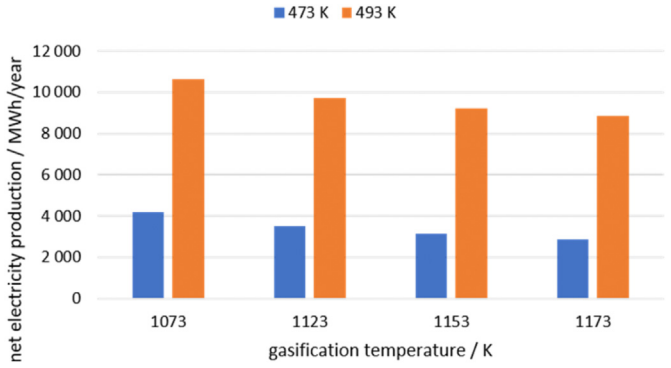

Fig. 7. Available excess electrical energy from FT offgas combustion and expansion in a gas turbine and after subtracting power needs in the BG-FT fuel production process.

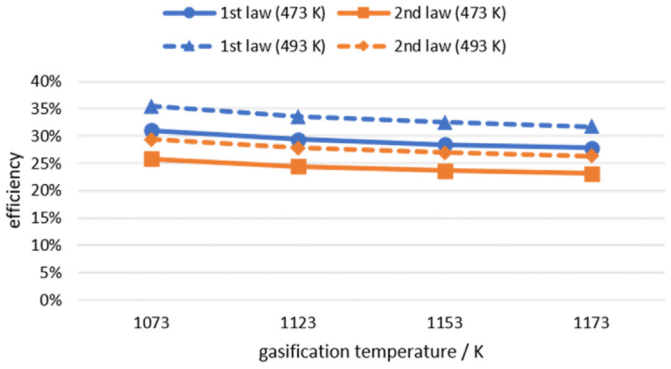

Fig. 8. 1st law (LHV) and 2nd law efficiencies of the FT biofuel production process including the generation of excess electrical energy as function of gasification temperature and temperature in the FT synthesis.

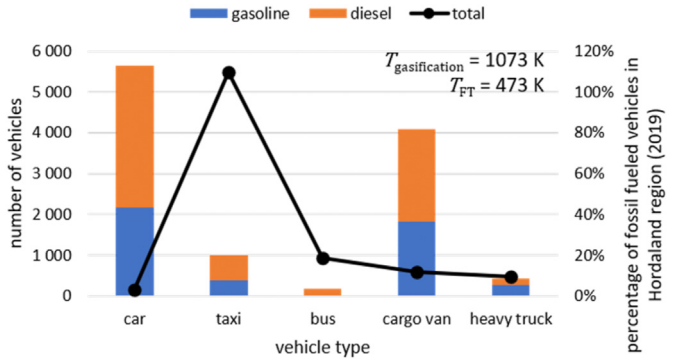

Fig. 9. Number of vehicles of different type and the percentage of that vehicle type registered in the Hordaland region which could be supplied with the produced FT biofuels.

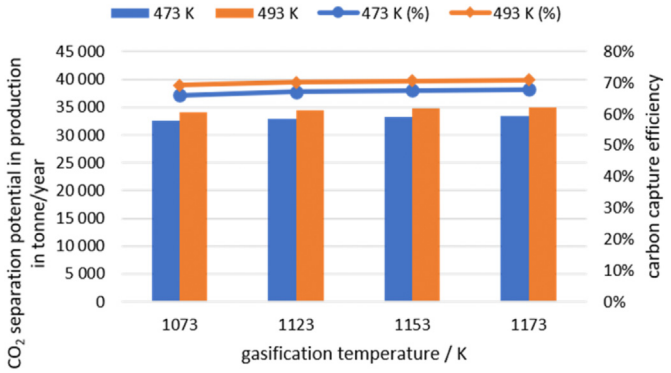

Fig. 10. Annual CO_2 separation potential in the FT biofuel production process (bars; left vertical axis) and the fraction of the carbon in the biomass that could be captured (lines; right vertical axis).

The second law efficiencies (equation (15)) are on the average 5–6% smaller than the first law efficiencies. The values range from 25.8% to 23.1% at 493 K FT reaction temperature and increasing gasification temperature (from 1073 K to 1173 K). The same trend is seen for a FT synthesis temperature of 493 K with values between 29.4% and 26.3% respectively.

The number of vehicles that could be supplied with the FT fuels produced is shown in Fig. 9 (left vertical axis), together with the percentage of such vehicles in the Hordaland region in Western Norway (right vertical axis). Values for average annual driving distance [31], average fuel consumption [32], CO_2 emissions [32], and number of vehicles of the different types [33,34] are taken from the respective databases freely available at Statistics Norway. It is assumed that the whole amount of FT fuel is used to supply a single type of vehicle when these numbers are calculated. Amongst the various vehicle types, it is the number of cars, which can be fuelled by FT biofuels, that is the greatest; however, it is only a small fraction of the registered cars in the region (3%). Treating all taxis as cars shows that is possible to supply the entire fleet of registered taxis in the region with the FT biofuels (110%). This implies, however, that the distribution of gasoline and diesel fuelled taxis needs to be appropriate to be able to consume the amount of FT gasoline and FT diesel that is produced. Alternatively, 20% of the registered buses (191 of 1020) in the region could be supplied and the FT gasoline used for another type of vehicle. The percentage of cargo vans and heavy trucks that could potentially operate on the FT fuels produced is even lower, 11.7% and 9.5% respectively. There is a greater number of cargo vans and they have a smaller fuel consumption compared with the heavy trucks; which are fewer in numbers, but have a higher fuel consumption. The diesel driven heavy trucks represent only 3.7% of the registered vehicles of this type.

Fig. 10 shows the amount of CO_2 that can be separated from both syngas and flue gases (left axis) during the production process as a function of gasification temperature and FT synthesis temperature. About 53% of the CO_2 can be captured from the syngas, the rest is from the flue gas (FT offgas) and char combustion. The lines in Fig. 10 show the fraction of the carbon that enters the production process as part of the biomass (right axis), which can be separated for storage and use. There is only a slight increase with gasification temperature, from 32,500 to 33,400 tonne per year at an FT temperature of 473 K; which corresponds to 66.1%–68.0% carbon capture efficiency, respectively. The values at 493 K are 500 tonne per year higher, which corresponds to 69.3%–70.9% carbon capture efficiency at the higher FT temperature. On the road, the vehicles supplied with the FT biofuels will still emit CO_2 (8000 tonne/year) although the carbon will have its origin in a renewable source.

4.2. Hydrogen production

The results for annual hydrogen production potential, first law (LHV) and second law efficiency, are shown in Table 6.

The maximum amount of hydrogen, which can be produced per year, is 2367 tonne at 1073 K. The production potential decreases with increasing gasifier temperature to 2210 tonne at 1173 K. First law and second law efficiencies for as produced (26 bar), compressed (350 bar) and liquefied hydrogen follow this trend with temperature. The first law efficiencies based on the LHV of both hydrogen and biomass are significantly over 50%, with the maximum value close to 60% for the hydrogen leaving the PSA unit at 26 bar. Compression to 350 bar leads to a drop in first-law efficiency by 1.2% ± 0.1%, on the average. The first law efficiency of liquid hydrogen production is roughly 10% lower than the first law efficiency for hydrogen at 26 bar, with the highest value at 47.7%.

Fig. 11, on the left axis, shows the number of vehicles of different types that could be supplied with the produced hydrogen if the fuel would be supplied to one vehicle type exclusively. The right axis in the same figure shows the fraction of registered vehicles of the respective type in the Hordaland region (2019), which today use fossil fuels, and which could be replaced by hydrogen fuelled vehicles. The numbers are based on the greatest possible amount of hydrogen able to be produced (at 1073 K gasification temperature). The replacement potential is greater for cars (20,831) followed by cargo vans (11,390), heavy trucks (981) and buses (656). The amount of hydrogen would be enough to supply four times the amount of registered taxis in the region (not shown in Fig. 11). Even though the number of cars, which could potentially be supplied with hydrogen, is quite large, it is only 9.9% of the registered cars in the Hordaland region. The most significant percentage effect for a vehicle type if converting their energy source from fossil fuel to hydrogen would be for buses, where 64.3% of the busses operating in the region could be run on hydrogen.

The carbon capture potential and efficiency of the hydrogen production process are shown on the left and right axis in Fig. 12, respectively. The total amount CO_2, which could be captured is almost independent of the gasification temperature. It is 45,978 tonne/year at 1073 K and 46,221 tonne/year at 1173 K. Consequently, the carbon capture efficiency is almost constant, ranging from 93.4% at 1073 K to 93.9% at 1173 K.

In contrast to using FT biofuels, there will be no more CO_2 emissions from the vehicles supplied when hydrogen is used as fuel. This leads to a further reduction potential in CO_2 emissions as shown in Fig. 13. It is largest for cars (34,000 tonne/year) followed by heavy trucks (29,819 tonne/year), cargo vans (24,973 tonne/

Table 6
Annual H_2 production potential and first law (LHV based) and second law efficiency of as produced (26 bar), compressed (350 bar) and liquefied hydrogen as function of gasification temperature.

$T_{gasifier}$ / K	m_{H_2} / tonne/year	$\eta_{LHV,26\ bar}$	$\eta_{LHV,350\ bar}$	$\eta_{LHV,\ liquid}$	$\eta_{II,\ 26\ bar}$	$\eta_{II,\ 350\ bar}$	$\eta_{II,\ liquid}$
1073	2367	58.1%	56.8%	47.7%	47.4%	47.9%	43.0%
1123	2288	56.1%	54.9%	46.3%	45.8%	46.3%	41.8%
1153	2243	54.9%	53.8%	45.6%	44.9%	45.4%	41.0%
1173	2210	54.1%	53.0%	45.0%	44.2%	44.7%	40.5%

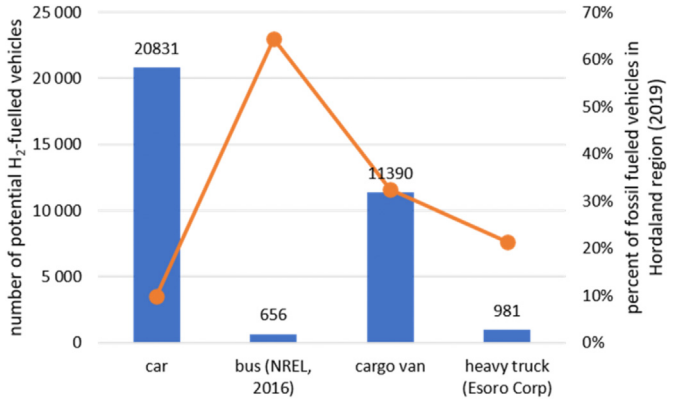

Fig. 11. Left axis: number of fossil-fuelled vehicles of different types that could be replaced by hydrogen-fuelled vehicles if the complete annual production at 1073 K was used by one specific vehicle type only. Right axis: fraction of vehicles registered in the Hordaland region (2019) which could be replaced.

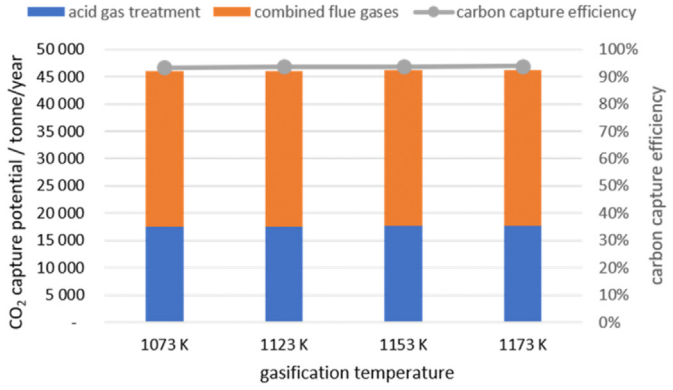

Fig. 12. Left axis: Annual CO_2 capture potential from the hydrogen production process from both syngas and the flue gases from char and PSA offgas combustion. Right axis: Fraction of biomass carbon content that can be captured as CO_2 from syngas and PSA offgas.

year) and busses (17,693 tonne/year). Combining the capture potential during production with the potentially avoided emissions from the vehicles leads to a maximum amount of 80,034 tonne per year (cars), which could be kept from entering the atmosphere, while the minimum amount would be 63,671 tonne/year (buses).

5 Discussion

The raw material entering the process is the wet organic fraction of municipal solid waste. Its composition is an average for the year 2013 and based on random samples taken that year [17,18]. Variations of the syngas composition and product yield are therefore to be expected in an actual realisation of the described processes. The calculation of syngas composition is based on an equilibrium process, which assumes a large enough reactor for this equilibrium to

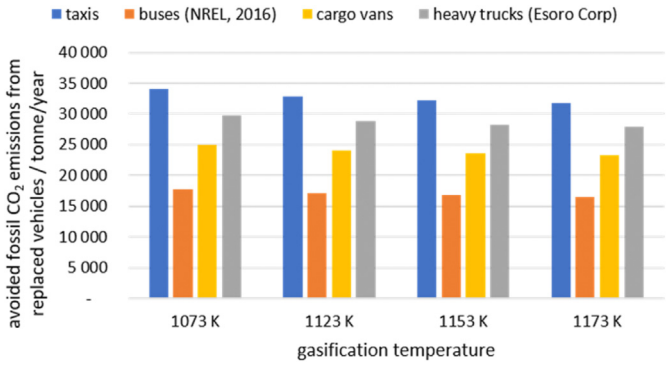

Fig. 13. Annual potential for avoiding CO_2 emissions when fossil-fuelled vehicles are replaced by hydrogen-fuelled vehicles.

be achieved. This is a further source for deviations in product yield that needs to be considered. Therefore, the calculated amount of both hydrogen and Fischer-Tropsch biofuels should be interpreted as an upper limit for what can be achieved in fuel production. The plant capacity in this work is much smaller compared with those in the reports by Spath et al. [8] and Swanson et al. [9]; but this should only have an impact on techno-economic calculations, not on calculations of production potential and efficiency.

The applied algorithm and method for syngas composition prediction has been developed further by including both ash in the reaction equation and energy balance, as well as several additional compounds on the product side, when compared to its first use in such calculations [5]. The inclusion of additional light hydrocarbons was suggested as further work in ref. [5] and implemented for this study. The RMSE calculated for the same conversion processes as used for validation in ref. [5] indeed show a slight improvement in accuracy. A recent model by Trninić et al. [35] divides the ideal reactor, which is assumed implicitly by the Gibbs free energy minimisation method, into three different zones for drying, pyrolysis, and gasification. This approach has shown to give good agreement between experimental and numerical results. Part of the future work to be conducted by the authors of this research will be the continued development their existing code in a similar direction.

There are other ways to calculate the chain growth factor α than used in this work, for example in the work by Im-orb et al. [12]. However, it is not clear in which unit the concentration of CO and H_2 needs to be given in the respective equation detailed in ref. [12]. Therefore, the equation from the report of Swanson et al. [9]. was used, as it can also be found in the work of Wang et al. [7]. The effect of different ways of calculating the chain growth factor could therefore not be investigated and considered.

The energy and exergy efficiencies obtained for both H_2 and FT biofuel products are for the case that all internal heat demand (biomass drying, syngas heating) in the respective processes can be provided by internal heat sources; such as heat from char combustion, both FT and PSA offgas combustion and syngas cooling.

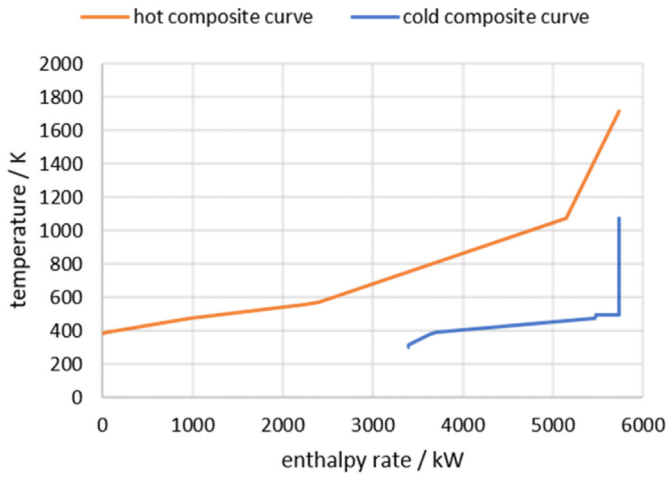

Fig. 14. Hot and cold composite curve for the Fischer-Tropsch fuel production process with syngas production at 1073 K in the gasifier and WGS reactor at 493 K.

This approach is valid because hot and cold composite curves for each of the production processes do not touch or cross over for a minimum pinch temperature difference of 5 K (and neither for reasonable values larger than that). This is shown by the hot and cold composite curves for the Fischer-Tropsch fuel production process in Fig. 14 and in Fig. 15 for hydrogen production, both at 1073 K gasification temperature. Both diagrams were made with help of a pinch analysis tool [36]. The heat demand for hydrogen production is larger due to the greater temperature for the high temperature water-gas shift reaction compared with the lower temperature in the case of Fischer-Tropsch fuel production. The diagrams show a large cooling demand of over 3.3 MW for the Fischer-Tropsch fuel production (Fig. 14) and over 5.5 MW for the hydrogen production process (Fig. 15), at 1073 K gasification temperature. The latter goes up to 6.1 MW at 1173 K gasification temperature. That this waste heat is mainly available in the temperature interval between 400 K and 600 K makes it suitable for recovery to electric energy by organic Rankine cycles, for example. An alternative is utilizing it as district heat which the nearby waste incineration facility is providing thermal energy to. The recovery of the waste heat would increase both energy and exergy efficiency to a certain degree as the exergy of this utilized excess heat would count as recovered exergy.

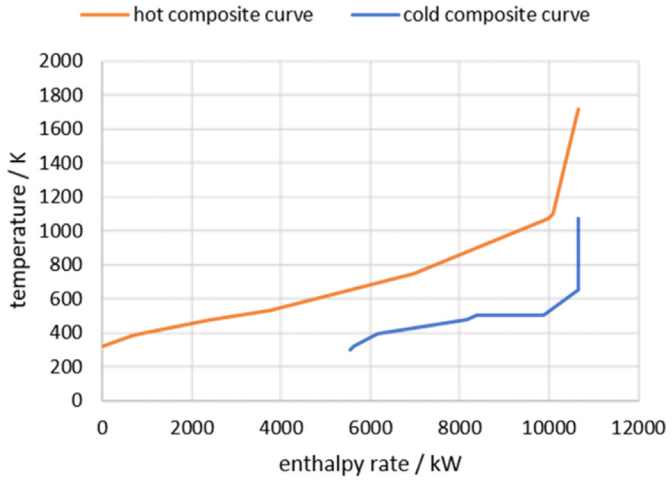

Fig. 15. Hot and cold composite curve for the hydrogen production process with syngas production at 1073 K in the gasifier.

The energy efficiency of the FT biofuel production in this work is lower compared with the values obtained by Swanson et al. [9]. According to the latter, the biomass to fuel efficiency is 39% and 43% when electricity production is added while it is 27.8% and 31.1% at 473 K FT synthesis temperature and 31.7% and 35.5% at 493 K FT synthesis temperature (including electricity production) in this work.

The exergy efficiencies are 5–6% smaller compared with the energy efficiencies, which is a typical difference. Values between 23.1% and 29.4% were found, depending on the specific combination of gasification and FT reaction temperature. These values are in good agreement with results obtained by Cruz et al. [15]. They determined exergy efficiencies in the same range (23.7%–26.7%) in their Aspen Plus based study of steam gasification (1143 K, 1.6 bar) of biomass (poplar) for FT fuel production at 493 K.

The fraction of biomass carbon converted to carbon in hydrocarbons in the liquid fuels and the wax fraction is ca. 26%. This is the same fraction as Swanson et al. obtained [9] and therefore the production potential is comparable in these two studies. The wax is not further processed in the current work. With annual amount can be up to 1220 tonne, which could give more additional fuel if cracked to shorter hydrocarbons, this could increase production of both gasoline and diesel fractions. The waxes may also be used for other purposes as there is a market for Fischer-Tropsch waxes. The wax fraction has not been considered in the calculation of both energy and exergy efficiencies. The produced wax is represented by triacontane ($C_{30}H_{62}$) in this study, which has a heating value that is about two orders of magnitude lower than that of both gasoline and diesel. Consequently, it would not change the numbers presented for energy and exergy efficiencies significantly.

Cruz et al. [15] obtained a mass of gasoline recovered per kg dry biomass was between $1.69 \cdot 10^{-2}$ $kg_{gasoline}/kg_{dry\ biomass}$ and $2.41 \cdot 10^{-2}$ $kg_{gasoline}/kg_{dry\ biomass}$ while the results in this study are between $3.75 \cdot 10^{-2}$ $kg_{gasoline}/kg_{dry\ biomass}$ and $4.18 \cdot 10^{-2}$ $kg_{gasoline}/kg_{dry\ biomass}$ at 493 K FT reaction temperature. The corresponding values for diesel are $4.41 \cdot 10^{-2}$ $kg_{diesel}/kg_{dry\ biomass}$ to $6.29 \cdot 10^{-2}$ $kg_{diesel}/kg_{dry\ biomass}$ by Cruz et al. while they are between $3.33 \cdot 10^{-2}$ $kg_{diesel}/kg_{dry\ biomass}$ and $3.57 \cdot 10^{-2}$ $kg_{diesel}/kg_{dry\ biomass}$ in this work respectively. The higher yield obtained by Cruz et al. may have several reasons. One is the lower ash content of the biomass (2.7 wt % vs. 25.9 wt% in this study). A further observation is the much larger CO/CO_2-ratio of 3.3 in the work of Cruz et al. [15] compared to this work, where it is just below 1.4. This means that much more carbon goes into the formation of CO, which is then available for the Fischer-Tropsch reaction compared to the process studied in this work. Others reasons may be the use of steam as the gasifying agent and hydrocracking the FT waxes for increased gasoline and diesel production.

Sues et al. studied the energy and exergy efficiency of five different biowaste-to-biofuel routes via gasification [37] with Aspen Plus process simulation software employing a Gibbs-type reactor for the gasification process. One of five biowaste types compared was municipal waste with a higher heating value of 16.5 MJ/kg while it is 15.4 MJ/kg in the current work. Energy efficiencies (based on the biowaste's higher heating value) of 38% for FT biofuel production and 59% for hydrogen production were found by Sues et al. [37]. The corresponding value in this work are 27.5%–24.7% with increasing gasification temperature for FT biofuels and 68.6%–64% for hydrogen production respectively. Although the FT biofuel production process used by Sues et al. is comparable, the municipal biowaste has a higher carbon content, which could be one reason for the larger energy efficiency they obtained. When comparing the mole fractions of the syngas produced by the gasification process, the mole fraction of CO is 15.8–15.0 vol% CO in this

study (1073 K–1173 K) while Sues et al. give a range of 23–27 vol% CO for air gasification in the temperature range 973 K–1173 K. The lower CO content in this work is likely to be the reason for a lower hydrocarbon yield and therefore a smaller energy efficiency. This will also explain the lower exergy efficiency of 29.4%–26.3% (at 220°C FT synthesis temperature) compared to 37% obtained by Sues et al. at 260°C FT synthesis temperature.

Sues et al. [37] used a steam gasification process for their hydrogen production process. It is therefore difficult to compare hydrogen and carbon monoxide mole fractions in the syngas from the gasifier. While their sum is larger than 80% in the steam gasification syngas, the air gasification approach used in this work yields only about 60%. Energy efficiencies of 68.6%–64% (with increasing gasification temperature) were obtained by the authors of this work, while 57% was the result published by Sues et al. The exergy efficiencies however are very close with 47.4%–44.2% (this work) and 48% (Sues et al.).

It is worth considering replacing air with oxygen as gasifying agent in the hydrogen production process as nitrogen has almost 50% mole fraction in the syngas prior to hydrogen separation by PSA. The oxygen could be provided by water electrolysis facilities to be established in the region where oxygen is a by-product of hydrogen production. Another possibility for further increase of the hydrogen partial pressure could be another step of CO_2 removal from the product gas flow. By removing these two compounds from the gas, the hydrogen mole fraction would be around 90%. However, another CO_2 removal step would increase cost while the oxygen from electrolysis plants could be cheap.

The results for hydrogen production potential and supply to road vehicles is more accurate compared to ref. [5]. The particulars considered in the production process are accounted for in greater detail compared with the assumption of simple conversion efficiencies for the water gas shift reaction and efficiency of hydrogen separation from the syngas. Like for the FT biofuels, both energy and exergy efficiency are calculated on this occasion based on the fuel and eventual excess electric energy (FT biofuels only) produced. This gives a better picture of the recovered energy in the main product(s) compared with the cold gas efficiency, for example, which measures the efficiency based on the energy and exergy content of the raw syngas.

The larger carbon capture potential when producing hydrogen compared with FT biofuels is not unexpected as the carbon is an integral part in the fuel. From the perspective of reducing carbon emissions, hydrogen production would be preferred over the production of FT biofuels as it also has better energy and exergy efficiencies. When using hydrogen as a fuel the consequence of implementing new infrastructure remains. It is still not in place in most locations where hydrogen is wanted as a zero-carbon-emissions fuel. The cost of this new infrastructure and the education of the people using it also needs consideration. Switching from liquid fossil to FT biofuels has obviously a lower barrier as more existing infrastructure can be used or modified for the new fuel; whilst changes in operations and maintenance of storage and supply and use in vehicles are almost negligible compared to the technology shift connected to hydrogen. Two things should therefore be studied in addition. One is the production cost of both fuels per unit mass of fuel and the comparison to production cost based on other methods. As previously mentioned, the biomass handling capacity of the proposed production processes is smaller than the capacity in the studies by Spath et al. [8] and Swanson et al. [9]. This can be expected to have an impact on the production cost leading to higher product cost per unit mass. The other aspects to study are the greenhouse gas emissions over the facilities' lifetimes and other environmental impacts of the produced fuels. The production process is only a part of the whole picture. For example, the construction and demolition of the production facility as well as distribution of the fuel need to be considered in an additional life cycle analysis.

Processing the wet organic waste separately from the overall waste at the current waste incineration facility in Bergen has not only the advantage that more waste can be processed in an area with increasing population. It has also the advantage of increased energy recovery as fuel in addition to heat, electricity (from waste) and biomethane (from sewage sludge). As more waste is processed, more carbon can be captured as CO_2. There are actually options for both use and permanent storage of CO_2 under development close to the place where the proposed hydrogen or FT biofuel production could be located.

The captured CO_2 can be stored permanently under the North Sea as part of the Northern Lights project currently under development close to Bergen, Norway [38]. Northern Lights is part of the national full-scale CCS project in which a complete value chain from capture to transport and storage is to be developed by 2024. The CO_2 could be transported either on land or by ship from the waste processing facility to the injection point at Kollsnes, about 55 km away.

Another use of the captured CO_2 is to turn it into carbon-based materials. A few years ago [39], the waste incineration plant in Bergen was among the 10 largest emitters of CO_2 in the region. In 2018, 225,000 tonne CO_2 were emitted to the atmosphere [40]. In order to reduce the emissions, the plant operator is planning to implement carbon capture from the flue gases in the near future. A pilot project to turn the carbon from the separated CO_2 into carbon fibres and nanomaterials is currently under development [41]. CO_2 captured from either hydrogen or FT biofuel production from organic waste would provide an additional input stream to the carbon-based material production facility and a possibility to create a revenue from the produced materials, like carbon nanotubes, for example.

6 Conclusion

This work compared the amount of different types of fuels that can be produced from the same synthesis gas produced by biomass gasification and their potential effect on CO_2 emission reduction from road traffic in the Hordaland region in Western Norway. The available wet organic waste mass of 35,843 dry tonne can either be turned into 2367 tonne hydrogen or 1233 tonne FT gasoline and 1627 tonne FT diesel with energy and exergy efficiencies comparable to state-of-the-art research in this field. From the processes studied, the number of fossil-fuelled vehicles that can potentially be replaced is found to be larger in the case of hydrogen production compared with production of Fischer-Tropsch biofuels. This is independent of the vehicle type that would be provided with the fuel. As more than 45,000 tonne CO_2 could be captured when producing hydrogen from the biowaste, a considerable amount of CO_2 could be prevented from entering the atmosphere. Storing it either underground or turning into carbon-based materials are two options, which will be locally available in the near future. As fossil-fuelled cars are more likely to be replaced with electric cars, reserving the produced hydrogen for heavy transport where up to 29,800 tonne CO_2 emissions from fossil fuels could be avoided per year, a considerable contribution to greenhouse gas emission reduction can be achieved in the Bergen and Hordaland region.

A further study on the production cost of both fuels needs to estimate if any of the proposed fuels can be competitive with other established or renewable solutions. Both the scale of the proposed facility and the current economic conditions in Norway will have an impact on this. It could also reveal if the recent purchase of a large number of buses powered by biodiesel was a good choice or if the

local public transport operator should have gone for hydrogen-fuelled models.

Credit author statement

Norbert Lümmen: Conceptualization, Methodology, Software, Validation, Formal analysis, Investigation, Resources, Data curation, Writing - original draft, Writing - review & editing, Visualization, Supervision, Project administration; Erlend Velken Røstbø; Methodology, Software, Validation, Formal analysis, Investigation, Writing - review & editing, Visualization

Declaration of competing interest

The authors declare that they have no known competing financial interests or personal relationships that could have appeared to influence the work reported in this paper.

Acknowledgements

This work was internally funded at Western Norway University of Applied Sciences (WNUAS). This research did not receive any specific grant from funding agencies in the public, commercial, or not-for-profit sectors. Erlend Velken Røstbø was a bachelor student in mechanical engineering at the Department of Mechanical and Marine Engineering at WNUAS. The authors are grateful to Prof. Richard J. Grant from the Department of Mechanical and Marine Engineering at WNUAS for checking the language in this manuscript. Thank you to Gerard Ayuso Virgili from the Department of Safety, Chemistry and Biomedical laboratory sciences at WNUAS for help with debugging the VLE calculations in Aspen One.

References

[1] Statistics Norway. *Emissions to air*. Available at: https://www.ssb.no/en/statbank/table/08940, accessed online: 22 June 2020.
[2] accessed online: Global Carbon Project. Global carbon Atlas. Available at: http://www.globalcarbonatlas.org/en/CO2-emissions. [Accessed 22 June 2020].
[3] accessed online: Office of the Prime Minister. A new and more ambitious climate policy for Norway. Available at: https://www.regjeringen.no/en/aktuelt/ny-og-mer-ambisios-klimapolitikk/id2393609/. [Accessed 23 June 2020].
[4] Statistics Norway. *Waste accounts*. Available at: https://www.ssb.no/en/statbank/table/10513, accessed online: 22 June 2020.
[5] Renkel MF, Lümmen N. Supplying hydrogen vehicles and ferries in Western Norway with locally produced hydrogen from municipal solid waste. Int J Hydrogen Energy 2018;43:2585–600.
[6] Wright MM, Daugaard DE, Satrio JA, Brown RC. Techno-economic analysis of biomass fast pyrolysis to transportation fuels. Fuel 2010;89:S2–10.
[7] Wang B, Gebreslassie BH, You F. Sustainable design and synthesis of hydrocarbon biorefinery via gasification pathway: integrated life cycle assessment and technoeconomic analysis with multiobjective superstructure optimization. Comput Chem Eng 2013;52:55–76.
[8] Spath P, Aden A, Eggeman T, Ringer M, Wallace B, Jechura J. Biomass to hydrogen production detailed design and economics utilizing the battelle columbus laboratory indirectly-heated gasifier. Report no. NREL/TP-510-37408. National Renewable Energy Laboratory; 2005.
[9] Swanson RM, Satrio JA, Brown RC, Platon A, Hsu DD. Techno-economic analysis of biofuels production based on gasification. National Renewable Energy Laboratory; 2010. Report no. NREL/TP-6A20-46587.
[10] Doranehgard MH, Samadyar H, Mesbah M, Haratipour P, Samiezade S. High-purity hydrogen production with in situ CO_2 capture based on biomass gasification. Fuel 2017;202:29–35.
[11] Howaniec N, Smoliński A. Effect of fuel blend composition on the efficiency of hydrogen-rich gas production in co-gasification of coal and biomass. Fuel 2014;128:442–50.
[12] Im-orb K, Simasatitkul L, Arpornwichanop A. Techno-economic analysis of the biomass gasification and Fischer–Tropsch integrated process with off-gas recirculation. Energy 2016;94:483–96.
[13] Im-orb K, Arpornwichanop A. Techno-environmental analysis of the biomass gasification and Fischer-Tropsch integrated process for the co-production of bio-fuel and power. Energy 2016;112:121–32.
[14] Barbuzza E, Buceti G, Pozio A, Santarelli M, Tosti S. Gasification of wood biomass with renewable hydrogen for the production of synthetic natural gas. Fuel 2019;242:520–31.
[15] Cruz PL, Iribarren D, Dufour J. Exergy analysis of alternative configurations of a system coproducing synthetic fuels and electricity via biomass gasification, Fischer-Tropsch synthesis and a combined-cycle scheme. Fuel 2017;194:375–94.
[16] Leibbrandt NH, Aboyade AO, Knoetze JH, Görgens JF. Process efficiency of biofuel production via gasification and Fischer–Tropsch synthesis. Fuel 2013;109:484–92.
[17] Harneshaug HK, Solheimslid T. Calculation of second law efficiency of energy recovery from waste [bachelor thesis]. Bergen, Norway: Bergen University College; 2014.
[18] Solheimslid T, Harneshaug HK, Lümmen N. Calculation of first-law and second-law-efficiency of a Norwegian combined heat and power facility driven by municipal waste incineration – a case study. Energy Convers Manag 2015;95:149–59.
[19] Nexant Inc. Equipment design and cost estimation for small modular biomass systems, synthesis gas cleanup, and oxygen separation equipment. Report no. NREL/SR-510-39945. National Renewable Energy Laboratory; 2006.
[20] Pal DB, Chand R, Upadhyay SN, Mishra PK. Performance of water gas shift reaction catalysts: a review. Renew Sustain Energy Rev 2018;93:549–65.
[21] Fournel S, Marcos B, Godbout S, Heitz M. Predicting gaseous emissions from small-scale combustion of agricultural biomass fuels. Bioresour Technol 2015;179:165–72.
[22] Jarungthammachote S, Dutta A. Equilibrium modeling of gasification: Gibbs free energy minimization approach and its application to spouted bed and spout-fluid bed gasifiers. Energy Convers Manag 2008;49:1345–56.
[23] Jarungthammachote S, Dutta A. Thermodynamic equilibrium model and second law analysis of a downdraft waste gasifier. Energy 2007;32:1660–9.
[24] Obernberger I, Brunner T, Bärnthaler G. Chemical properties of solid biofuels—significance and impact. Biomass Bioenergy 2006;30:973–82.
[25] European Commision. Integrated pollution prevention and control. Reference document for the best available techniques for waste incineration. European commission. Retrieved from. 2006. http://eippcb.jrc.ec.europa.eu/reference/BREF/wi_bref_0806.pdf. [Accessed 27 June 2017].
[26] McBride BJ, Gordon S, Reno MA. Coefficients for calculating thermodynamic and transport properties of individual species. NASA (national aeronautics and space administration). Report no. 4513. 1993.
[27] Altafini CR, Wander PR, Barreto RM. Prediction of the working parameters of a wood waste gasifier through an equilibrium model. Energy Convers Manag 2003;44:2763–77.
[28] Bell IH, Wronski J, Quoilin S, Lemort V. Pure and Pseudo-pure fluid thermophysical property evaluation and the open-source thermophysical property library CoolProp. Ind Eng Chem Res 2014;53:2498–508.
[29] Lümmen N, Karouach A, Tveitan S. Thermo-economic study of waste heat recovery from condensing steam for hydrogen production by PEM electrolysis. Energy Convers Manag 2019;185:21–34.
[30] Aasadnia M, Mehrpooya M. Large-scale liquid hydrogen production methods and approaches: a review. Appl Energy 2018;212:57–83.
[31] Statistics Norway. Road traffic volumes. Available at: https://www.ssb.no/en/statbank/table/12576/, accessed online: 22 June 2020.
[32] Statistics Norway. Utvalgte faktorer for mobile utslipp til luft etter kilde. Utslipp per kjørte kilometer. 2016 (english: Selected factors for mobile emissions to air by source. Emissions per kilometer driven. 2016). Available at: https://www.ssb.no/natur-og-miljo/artikler-og-publikasjoner/hva-pavirker-utslipp-til-luft-fra-veitrafikk?tabell=318157. [Accessed 22 June 2020].
[33] accessed online: Statistics Norway. Registered vehicles. Available at: https://www.ssb.no/en/statbank/table/11823. [Accessed 22 June 2020].
[34] accessed online: Statistics Norway. Taxi transport. Available at: https://www.ssb.no/en/statbank/table/11271/. [Accessed 22 June 2020].
[35] Trninić M, Stojiljković D, Manić N, Ø Skreiberg, Wang L, Jovović A. A mathematical model of biomass downdraft gasification with an integrated pyrolysis model. Fuel 2020;265:116867.
[36] accessed online: Umbach JS. Online pinch analysis tool. Available at: www.uic-che.org/pinch. [Accessed 9 September 2020].
[37] Sues A, Juraščík M, Ptasinski K. Exergetic evaluation of 5 biowastes-to-biofuels routes via gasification. Energy 2010;35:996–1007.
[38] accessed online: CCS Norway. Northern lights CCS - about the project. Available at: https://northernlightsccs.com/en/about. [Accessed 30 August 2020].
[39] Hordaland fylkeskommune. Handlingsprogram 2019 - klimaplan for Hordaland 2014-2030. 2019. https://www.hordaland.no/globalassets/for-hfk/natur-og-klima/8-11-klimaplanen-sitt-handlingsprogram-2019.pdf. [Accessed 9 September 2020].
[40] accessed online: BIR AS. Årsrapport. Bergen, Norway. 2019. Retrieved from, https://bir.no/media/10412/aarsrapport_2018.pdf. [Accessed 9 September 2020].
[41] Naturpress. I Bergen skal CO_2 fanges og bli til karbon-nanofiber (english: In Bergen, CO_2 is to be captured and turned into carbon nanofibres). Available at: https://www.naturpress.no/2019/01/10/i-bergen-skal-co2-fanges-og-bli-til-karbon-nanofiber/, accessed online: 2 July 2020.